J Mater Sci: Mater Med (2007) 18:1825–1829
DOI 10.1007/s10856-007-3036-3

Preparation of porous hydroxyapatite with interconnected pore architecture

Hui Gang Zhang · Qingshan Zhu

Received: 27 November 2005 / Accepted: 5 May 2006 / Published online: 5 May 2007

Abstract Since pore connectivity has significant effects on the biological behaviors of biomedical porous hydroxyapatite (PHA), the preparation of PHA with interconnected pore architecture is of great practical significance. In the present study, PHA with highly interconnected architecture was prepared via a simple burnout route with rod-like urea as the porogen. Microscopy and porosimetry data showed that the as-prepared PHA had open and interconnected pore structure with the average fenestration size of about 120 μm. Open pores occupied up to 98% of the total porosity. The compressive strength and modulus of the as-prepared PHA were respectively 1.3–7.6 MPa and 4.0–10.4 GPa.

Introduction

It is well known that vertebrate bones are mainly composed of highly interconnected hard inorganic mineral (hydroxyapatite) and soft organic components. The excellent properties of natural bones have attracted many attempts to mimic the interconnected frame structure. Thus, synthetic porous hydroxyapatite (PHA) ceramics with interconnected architecture have been widely investigated as osseous defect fillers and tissue engineering scaffolds. Considerable *in vivo* investigation showed that the internal architecture of PHA had the significant influence upon the implant effects [1, 2] and that a minimum pore size of approximately 100–150 μm is necessary for the continuous health of bony in-growth [3, 4]. The degree of interconnectivity is considered as the main limiting factor of osteoconduction rather than the size of the pores [2]. Therefore, the design of hydroxyapatite (HA) materials with highly interconnected pores [3, 5] and appropriate mechanical properties is necessary for maximizing the functions and *in vivo* properties of porous implants. Up to now, the preparation of highly interconnected pore structure still remains one of the major challenges for porous hydroxyapatite biomaterials [5, 6].

Various routes have been developed for PHA preparation, typically including incorporation of porogen particles [7–10], gel casting of foams [11], replication of a polymer sponge [12], solid freeform fabrication (SFF) [13], and salt leaching [14], etc. Their advantages and disadvantages have been discussed in the literature [6]. Of the above routes, the incorporation of porogens is the simplest, inexpensive and frequently used method, but previous reports showed that the incorporation of porogen particles usually led to closed and poorly interconnected pores [1, 12, 15], which is unfavorable to the bony in-growth. If porous hydroxyapatite with interconnected pore architecture can be prepared by using this simple method, it will be of great value and interest.

In this study, we prepared PHA bioceramics with interconnected pore architecture via a rod-like urea burnout route. Various properties of the as-prepared PHA were characterized by scanning electron microscopy (SEM), mercury porosimetry, etc. The influence of the preparation conditions upon PHA structure was also investigated.

H. G. Zhang · Q. Zhu (✉)
Multiphase Reaction Laboratory, Institute of Process Engineering, Chinese Academy of Sciences, P.O. Box 353, Beijing 100080, P.R. China
e-mail: qszhu@home.ipe.ac.cn

H. G. Zhang
Graduate School of the Chinese Academy of Sciences, Beijing 100039, P.R. China

Experimental

Preparation of HA powders

All chemical reagents used in this study were analytical grade and purchased from Beijing Chemicals Corp., China. Aqueous solutions of calcium acetate and di-ammonium hydrogen phosphate, with a Ca/P molar ratio of 1.67, were simultaneously added into 70 °C deionized water. Ammonia hydroxide was used to adjust the pH value of the solution to 10. After aging for 2 days at ~70 °C, the white precipitate was filtered with a Buchner funnel, and then dried in an air oven at 60 °C overnight. The morphology of the precipitate was observed by a field emission scanning electron microscope (FESEM, JSM-6700F, JEOL, Japan). The phase identification was performed with an X-ray diffractometer (XRD, X'Pert Pro, PAnalytical, The Netherland) with Cu$K\alpha$ radiation at a scanning rate of 20°/min. The Ca/P molar ratio was analyzed using inductively coupled plasma-atomic emission spectroscopy (ICP-AES, Analyst 200, Perkin–Elmer, USA).

Preparation of PHA ceramics

Rod-like urea particles, with ~200 μm in diameter and ~2 mm in length, were used as the porogen. The appropriate amounts of urea particles and hydroxyapatite powders were dry-mixed carefully and then die-pressed uniaxially at the pressure of 50 MPa to form cylindrical samples. The urea/HA weight ratios of five samples used were 0.75, 1, 1.5, 2, and 2.75, which corresponded to the urea volume content, 64.0%, 70.3%, 78.0%, 82.5%, and 86.7%, in the green bodies. These samples were heated to 500 °C at a heating rate of 0.2 °C/min to drive off the urea particles, followed by an increase to 1200 °C at a rate of 1 °C/min, and held for 2 h at 1200 °C. At last, the furnace was cooled down to 500 °C at a rate of 5 °C/min, and then naturally down to room temperature. Porogens with different morphologies were also attempted for comparison via the same processing route.

The morphology of the as-prepared PHA was observed by a scanning electron microscope (JSM-35CF, JEOL, Japan). The interpore connection distribution of the as-prepared PHA was determined by mercury porosimetry (AutoPore IV 9500, Micrometrics, USA). To determine the open porosity, samples were immersed in and fully filled by molten paraffin with the known density and afterwards solidified in air. Open pore volume can be calculated by the mass increase and the total volume was obtained by the Archimedean method.

Compression tests were performed using a universal testing machine (WDW-10, Tian Cheng Testing Machine Corp., China) fitted with a 10 kN load cell. The crosshead speed was controlled at 0.2 mm/min by a computer and the load was applied until samples were cracked. The elastic modulus was calculated by the slope of the initial linear portion of stress–strain curves. All the measurements were performed using at least five samples prepared under the same experimental conditions.

Results and discussion

Characteristics of synthetic HA powders

The XRD pattern of the as-prepared HA powder is illustrated in Fig. 1. All peaks fitted well with the standard HA diffraction pattern (JCPDS, #9-432). The broad peak width of the diffraction pattern could be attributed to the small crystal size, from which the average crystal size was coarsely estimated to be about 90 nm. ICP-AES analyses showed that the Ca/P molar ratio was 1.65, close to the stoichiometric ratio of 1.67. Figure 2 shows the FESEM image of the as-prepared HA powder, which revealed that most of the HA particles agglomerated together with the particle size ranged from 80–300 nm.

Characteristics of PHA ceramics

Figure 3 shows the SEM images of the samples prepared with different urea contents in green bodies. The pore content of the samples rose clearly with the increase of the starting urea amount in the green bodies. The average diameter of pores was coarsely estimated to be ~180 μm. The long channels in the images were due to the burnout of urea rods. Figure 3(f) demonstrates that the samples prepared via the rod-like urea burnout route possessed large fenestrations between two adjacent pores, which are

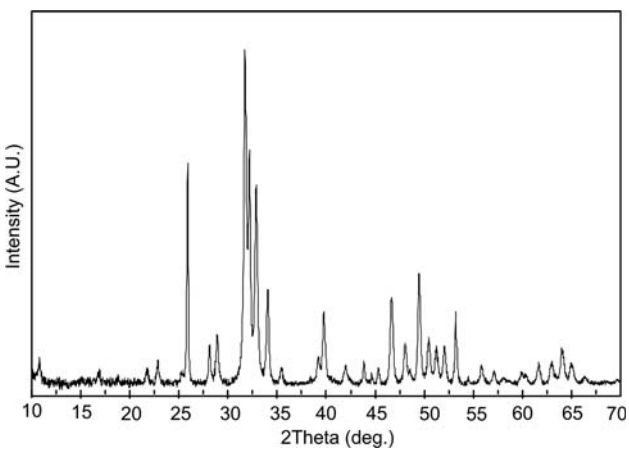

Fig. 1 XRD pattern of the as-prepared HA powder

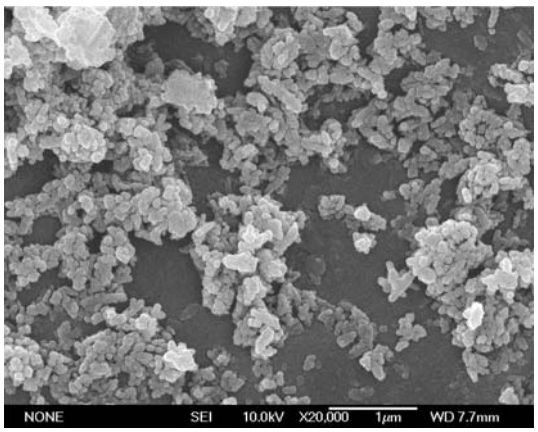

Fig. 2 FESEM image of the as-prepared HA powder

essential for osteoconductivity. If the fenestrations are too small, the growing cells may very likely block the 'windows' between the adjacent pores, which may cause the death of the cells located in the central portion of the scaffold because of a lack of nutrients [6].

The theoretical densities of dense HA and urea were assumed to be 3.156 and 1.335 g cm^{-3} respectively. The variations of the total and open porosities with the urea content are shown in Fig. 4. It can be seen that the close porosity occupied a relatively small fraction even in the low urea content range and the open pore percentage rose with the increase of the urea content. When the volume content of urea in the green body approached 86%, almost 98% pores were open. SEM images and porosity data suggested that the pores in the as-prepared PHA ceramics via the rod-like urea burnout route are highly interconnected.

The sintered sample with the urea/HA weight ratio of 1.5 (78.0 vol% urea) in the green body was subjected to mercury porosimetry. The result of incremental intrusion in Fig. 5 showed that most of the interpore connections ranged from 80 μm to 200 μm in diameter, with a maximum peak at 120 μm. The enlarged graph of 0.01–10 μm range showed a very low fraction of small pores with the neck diameter of 0.1–1 μm, which were mainly distributed

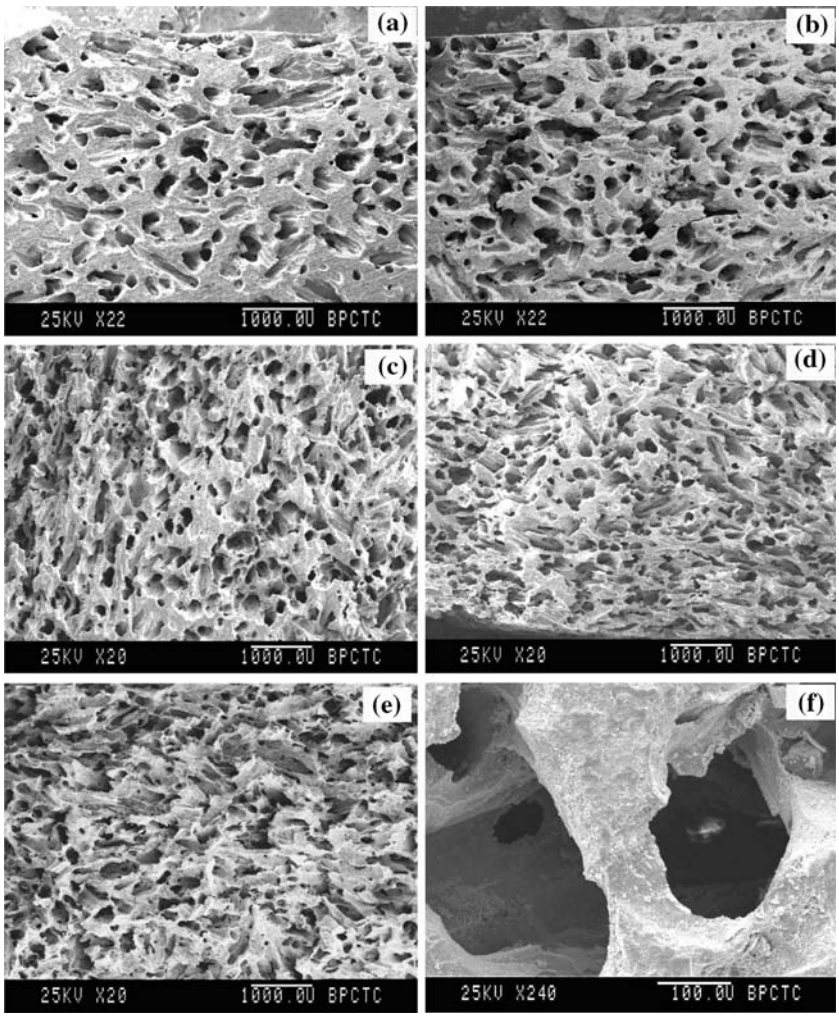

Fig. 3 SEM images of the PHA ceramics prepared with the different urea volume content in the green bodies; (**a**) 64.0%, (**b**) 70.3%, (**c**) 78.0%; (**d**) 82.5%; (**e**) 86.7%; (**f**) high magnification of the sample with 82.5% urea

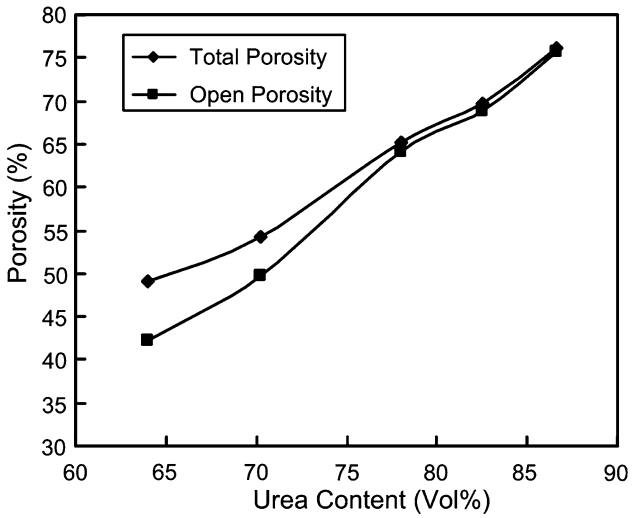

Fig. 4 Total and open porosity of PHA samples measured by the Archimedean method

on the wall and struts of macropores, These results were consistent with the observations made in SEM analysis and further confirmed that the pores obtained were interconnected.

PHA samples with a nominal dimension of about $\Phi 9 \times 10$ mm^3 were prepared to determine the compressive strength in a universal testing machine. Samples were placed between two pieces of thin artificial rubber sheets in order to avoid non-uniform loading. After the samples were loaded up to fracture at a constant crosshead speed, the elastic modulus on compression was calculated from the relationship between the stress and strain at the initial portion of the curves after disregarding the rubber sheet deformation. Results were based on the average value of at least five samples for each ratio of HA to urea. As shown in Fig. 6, the compressive strength of the sintered PHA ceramic via the rod-like urea burnout route varied within the range of 1.3–7.6 MPa and decreased with increasing urea content in green bodies. Similar trends were observed for the compressive modulus, which varied from 4.0 GPa to 10.4 GPa. Such mechanical properties were in the range of these of the cancellous bone (1–12 MPa) [16].

In the burnout route, two main processing parameters influence the properties of PHA significantly. One is the geometry of porogens including size and shape, which determines the morphologies of the resultant pores. Although from the literature [1, 12, 15] and the resulting images of previous reports [7, 8] using the method of incorporation of combustible porogens, it is generally admitted that this method would lead to blind and isolated pore structure. However, our results showed that the highly interconnected PHA could be successfully prepared with rod-like urea as the porogen. The reason may be that the rod-like shape provided more possibility for particles to overlap with each other by heads and tails, when samples

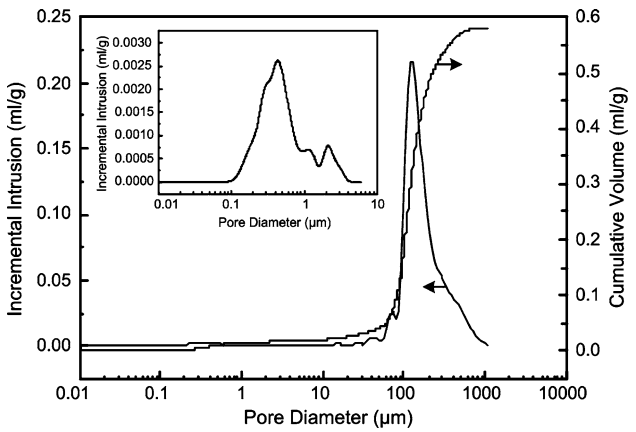

Fig. 5 Mercury intrusion curve of the sample containing 78.0 vol% urea in the green body

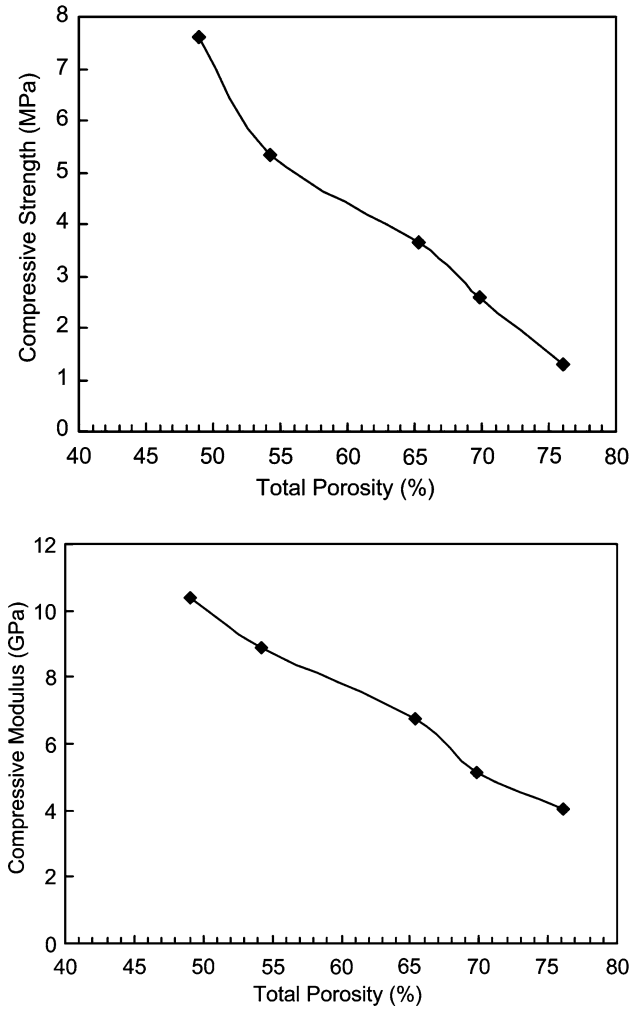

Fig. 6 Variations of the compressive strength and modulus with the total porosity

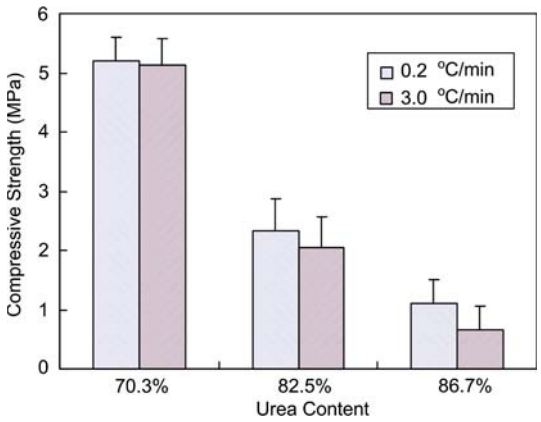

Fig. 7 Comparison of the compressive strength of PHA ceramics prepared at different heating rates

were pressed. After being burned out, the overlapped parts formed interconnected channels. By virtue of intuition, it seemed that longer rods might be more helpful to realize good connection in the low content of porogens. However, experiments using nylon rods with ~300 μm in diameter and ~5 mm in length led to delamination when sintering, which resulted from the rearrangement and orientation of longer rods along the plane perpendicular to the pressing force during die-pressing. Therefore, the rod length should be properly chosen, a length of around 2 mm seemed to be appropriate.

The heating rate is another important processing parameter, which affects the mechanical properties of the sintered PHA. Figure 7 is the comparison results of the effect of different heating rates on the compressive strength. It showed that in the case of low porogen content, the different heating rates, 0.2 °C/min and 3.0 °C/min, hardly resulted in much difference of compressive strength, but with the increase of the urea content, the influence of heating rates upon the compressive strength became significant. High heating rates apparently degraded the compressive strength of sintered PHA ceramics. Especially, when the weight ratio of urea to HA was larger than 2.75, the heating rate over 5 °C/min caused samples to collapse completely. The reason may be that the pores' wall and struts of PHA body were not fully densified when porogens were burn out, so the high heating rate resulted in the fast decomposition of urea particles and quick gas evolution destroyed the undensified porous framework, which was more significant in the high urea content. So the heating rate should be carefully controlled under 0.2 °C/min for the urea burnout route, in order to obtain better mechanical properties.

Conclusion

The PHA ceramics with highly interconnected pores were successfully fabricated by a simple rod-like urea burnout route. Characterization by SEM, Archimedean method and mercury porosimetry showed that the prepared pores were highly interconnected and the fenestrations between two adjacent pore channels had the average diameter of about 120 μm, which would be very helpful to the flow of nutrients and the healthy growth of cells. The compressive strength of the prepared PHA ranged from 1.3 MPa to 7.6 MPa, which is comparable to that of the cancellous bones. Therefore, the prepared porous hydroxyapatite would be appropriate materials for medical implant and tissue engineering scaffolds.

Acknowledgements We thank the financial support from the National Natural Science Foundation of China (No. 20221603) and Chinese Academy of Sciences.

References

1. T. M. G. CHU, D. G. ORTON, S. J. HOLLISTER, S. E. FEINBERG and J. W. HALLORAN, *Biomaterials* **23** (2002) 1283
2. B. S. CHANG, C. K. LEE, K. S. HONG, H. J. YOUN, H. S. RYU, S. S. CHUNG, K. and W. PARK, *Biomaterials* **21** (2000) 1291
3. K. A. HING, S. M. BEST and W. BONFIELD, *J. Mater. Sci: Mater. Med.* **10** (1999) 135
4. H. W. KIM, S. Y. LEE and C. J. BAE, *Biomaterials* **24** (2003) 3277
5. A. TAMPIERI, G. CELOTTI, S. SPRIO, A. DELCOGLIANO and S. FRANZESE, *Biomaterials* **22** (2001) 1365
6. S. H. LI, J. R. WIJIN, P. LAYROLLE and K. DE GROOT, *J. Am. Ceram. Soc.* **86** (2003) 65
7. D. M. LIU, *J. Mater. Sci: Mater. Med.* **8** (1997) 227
8. D. M. LIU, *J. Mater. Sci. Lett.* **15** (1996) 419
9. N. Ö. ENGIN and A. C. TAS, *J. Am. Ceram. Soc.* **83** (2000) 1581.
10. A. ŚLÓSARCZYK, E. STOBIERSKA and Z. PASZKIEWICZ, *J. Mater. Sci. Lett.* **18** (1999) 1163
11. P. SEPULVEDA, F. S. ORTEGA, M. D. M. INNOCENTINI and V. C. PANDOLFELLI, *J. Am. Ceram. Soc.* **83** (2000) 3021
12. H. R. RAMAY and M. Q. ZHANG, *Biomaterials* **24** (2003) 3293
13. J. M. TABOAS, R. D. MADDOX, P. H. KREBSBACH and S. J. HOLLISTER, *Biomaterials* **24** (2003) 181
14. D. TADIC, F. BECKMANN, K. SCHWARZ and M. EPPLE, *Biomaterials* **25** (2004) 3335
15. T. M. G. CHU, J. W. HALLORAN, S. J. HOLLISTER and S. E. FEINBERG, *J. Mater. Sci.: Mater. Med.* **12** (2001) 471
16. R. B. MARTIN, M. W. CHAPMAN, N. A. SHARKEY, S. L. ZISSIMOS, B. BAY and E. C. SHORS, *Biomaterials* **14** (1993) 341